

Jäger · Rannacher · Warnatz (Eds.)  
Reactive Flows, Diffusion and Transport

---

Willi Jäger · Rolf Rannacher · Jürgen Warnatz  
*Editors*

# Reactive Flows, Diffusion and Transport

**From Experiments via Mathematical Modeling  
to Numerical Simulation and Optimization**

Final Report of SFB  
(Collaborative Research Center) 359

With 293 Figures, 200 in Color, and 39 Tables

 Springer

*Editors*

Willi Jäger  
Rolf Rannacher  
Jürgen Warnatz

Interdisziplinäres Zentrum  
für Wissenschaftliches Rechnen (IWR)  
Universität Heidelberg  
Im Neuenheimer Feld 368  
69120 Heidelberg, Germany  
*jaeger@iwr.uni-heidelberg.de*  
*rannacher@iwr.uni-heidelberg.de*  
*warnatz@iwr.uni-heidelberg.de*

Library of Congress Control Number: 2006933613

Mathematics Subject Classification (2000): 92-XX, 76-XX, 85-XX, 35-XX, 49-XX, 65-XX

ISBN-10 3-540-28379-X Springer Berlin Heidelberg New York  
ISBN-13 978-3-540-28379-9 Springer Berlin Heidelberg New York

This work is subject to copyright. All rights are reserved, whether the whole or part of the material is concerned, specifically the rights of translation, reprinting, reuse of illustrations, recitation, broadcasting, reproduction on microfilm or in any other way, and storage in data banks. Duplication of this publication or parts thereof is permitted only under the provisions of the German Copyright Law of September 9, 1965, in its current version, and permission for use must always be obtained from Springer. Violations are liable for prosecution under the German Copyright Law.

Springer is a part of Springer Science+Business Media  
[springer.com](http://springer.com)

© Springer-Verlag Berlin Heidelberg 2007

The use of general descriptive names, registered names, trademarks, etc. in this publication does not imply, even in the absence of a specific statement, that such names are exempt from the relevant protective laws and regulations and therefore free for general use.

Typesetting by the editors using a Springer T<sub>E</sub>X macro package  
Production: LE-T<sub>E</sub>X Jelonek, Schmidt & Vöckler GbR, Leipzig  
Cover design: WMXDesign GmbH, Heidelberg

Printed on acid-free paper 46/3100/YL - 5 4 3 2 1 0

---

## Preface

This volume contains a series of articles which present new developments in the mathematical modeling, numerical simulation and optimization as well as the experimental characterization of complex processes in Physical Chemistry, Astrophysics and Environmental Physics.

The presented results have grown out of work done in the *Sonderforschungsbereich 359* (SFB 359) ‘Reactive Flow, Diffusion and Transport’ at the University of Heidelberg in which mathematicians, chemists and physicists collaborated on developing new methods for a better understanding of complex chemical and physical processes. The long-standing support by the German Research Foundation (DFG) is gratefully acknowledged.

The SFB 359 was established 1993 under the umbrella of the Interdisciplinary Center for Scientific Computing (IWR) and ended on December 31, 2004. It had about 100 members, i.e., senior scientists, post-docs and PhD students, who belonged to 10 of the 32 research groups of IWR. The research program of SFB 359 concentrated on mathematically based models for physical and chemical processes which share the difficulty of interacting diffusion, transport and reaction. Typical examples from Physical Chemistry are chemical reactions in flow reactors and catalytic combustion at surfaces, both requiring the consideration of multidimensional mass transport. In Astrophysics realistic modelling of star formation involves diffusive mass transport, energy radiation, and detailed chemistry. Processes of similar complexity occur in Environmental Physics in modeling pollutant transport in soil and waters. The central goal has been the development of solution methods for such problems which are theoretically supported and generally applicable.

According to the research program of SFB 359 the articles in this volume are organized in chapters as follows:

### *I. Mathematical analysis for transport-reaction systems*

The articles in the first chapter deal with the analysis of fluid flows and free boundaries, and nonlinear evolution processes, including geometry aspects.

*II. Navier-Stokes equations and chemical reactions*

In the second chapter new numerical approaches are described for solving multidimensional reactive flow problems by adaptive finite element methods with emphasis on mesh and model adaptivity combined with multigrid techniques and parallel processing.

*III. Optimization methods for reactive flows*

The third chapter presents new developments in numerical optimal control, e.g., robust parameter estimation, optimal experimental design, partially reduced SQP methods, and adaptive finite element methods for PDE-constrained optimal control problems.

*IV. Chemical reaction systems*

The fourth chapter is concerned with numerical and experimental methods for the determination of kinetic parameters in laminar flow reactors, and the characterization and optimization of reactive flows in catalytic monoliths and on catalytically active surfaces.

*V. Turbulent flow and combustion*

The articles in the fifth chapter present results of the numerical simulation of turbulent flows by a multigrid LES method, of turbulent non-reacting and reacting spray flows, and of transport and diffusion processes in boundary layers of turbulent channel flow.

*VI. Diffusion and transport in accretion discs*

The sixth chapter deals with the evolution of proto-planetary disks including detailed chemistry and mineralogy and the efficient numerical solution of multidimensional radiative transfer problems.

*VII. Flows in porous media*

In the seventh chapter analytical and computational multiscale methods are presented for treating reactive flows in porous media and boundary and interface processes. An application is lake dynamics which involves the numerical simulation and experimental study of unsaturated water flow in heterogeneous systems.

*VIII. Computer visualization*

This last chapter contains descriptions of software tools for the computer visualization of numerical data resulting from computer simulations: the interactive VTK-based graphics packages HiVision and VisuSimple, and a tool for efficient volume rendering in scientific applications.

Heidelberg,  
September 2006

*Willi Jäger  
Rolf Rannacher  
Jürgen Warnatz*

---

# Contents

---

## Part I Mathematical Analysis for Transport-Reaction Systems

---

**Preamble** ..... 3

### **Fluid Flows and Free Boundaries**

*B. Schweizer, S. Bodea, C. Surulescu, I. Suroutsova* ..... 5

### **Nonlinear Evolution Equations and Applications**

*W. Jäger, Th. Lorenz, A. Tambulea* ..... 25

---

## Part II Navier-Stokes Equations and Chemical Reactions

---

**Preamble** ..... 45

### **Mesh and Model Adaptivity for Flow Problems**

*R. Becker, M. Braack, R. Rannacher, T. Richter* ..... 47

### **Parallel Multigrid on Locally Refined Meshes**

*R. Becker, M. Braack, T. Richter* ..... 77

### **Solving Multidimensional Reactive Flow Problems with Adaptive Finite Elements**

*M. Braack, T. Richter* ..... 93

---

## Part III Optimization Methods for Reactive Flows

---

**Preamble** ..... 115

<b>Robustness Aspects in Parameter Estimation, Optimal Design of Experiments and Optimal Control</b> <i>H. G. Bock, S. Körkel, E. Kostina, J. P. Schlöder</i> .....	117
<b>Multiple Set Point Partially Reduced SQP Method for Optimal Control of PDE</b> <i>H. G. Bock, E. Kostina, A. Schäfer, J. P. Schlöder, V. Schulz</i> .....	147
<b>Adaptive Finite Element Methods for PDE-Constrained Optimal Control Problems</b> <i>R. Becker, M. Brauck, D. Meidner, R. Rannacher, B. Vexler</i> .....	177
<hr/>	
<b>Part IV Chemical Reaction Systems</b>	
<hr/>	
<b>Preamble</b> .....	209
<b>Determination of Kinetic Parameters in Laminar Flow Reactors. I. Theoretical Aspects</b> <i>T. Carraro, V. Heuveline, R. Rannacher</i> .....	211
<b>Determination of Kinetic Parameters in Laminar Flow Reactors. II. Experimental Aspects</b> <i>A. Hanf, H.-R. Volpp, J. Wolfrum</i> .....	251
<b>Optimization of Reactive Flows in a Single Channel of a Catalytic Monolith: Conversion of Ethane to Ethylene</b> <i>H. G. Bock, O. Deutschmann, S. Körkel, L. Maier, H. D. Minh, J. P. Schlöder, S. Fischer, J. Warnatz</i> .....	291
<b>Reaction Processes on Catalytically Active Surfaces</b> <i>O.R. Inderwildi, D. Starukhin, H.-R. Volpp, D. Lebiez, O. Deutschmann, J. Warnatz</i> .....	311
<b>Stochastic Modeling and Deterministic Limit of Catalytic Surface Processes</b> <i>J. Starke, C. Reichert, M. Eiswirth, K. Oelschläger</i> .....	341
<hr/>	
<b>Part V Turbulent Flow and Combustion</b>	
<hr/>	
<b>Preamble</b> .....	373
<b>Multigrid Methods for Large-Eddy Simulation</b> <i>A. Gordner, S. Nägele, G. Wittum</i> .....	375

**Modeling and Simulation of Turbulent Non-Reacting and Reacting Spray Flows**  
*H.-W. Ge, D. Urzica, M. Vogelgesang, E. Gutheil* ..... 397

**Transport and Diffusion in Boundary Layers of Turbulent Channel Flow**  
*S. Sanwald, J. v. Saldern, U. Riedel, C. Schulz, J. Warnatz, J. Wolfrum* 419

**Part VI Diffusion and Transport in Accretion Discs**

**Preamble** ..... 435

**Evolution of Protoplanetary Disks Including Detailed Chemistry and Mineralogy**  
*H.-P. Gail, W. M. Tscharnuter*..... 437

**Numerical Methods for Multidimensional Radiative Transfer**  
*E. Meinköhn, G. Kanschat, R. Rannacher, R. Wehrse* ..... 485

**Part VII Flows in Porous Media**

**Preamble** ..... 529

**Multiscale Analysis of Processes in Complex Media**  
*W. Jäger, M. Neuss-Radu*..... 531

**Microscopic Interfaces in Porous Media**  
*W. Jäger, B. Schweizer* ..... 555

**High-Accuracy Approximation of Effective Coefficients**  
*N. Neuss*..... 567

**Numerical Simulation and Experimental Studies of Unsaturated Water Flow in Heterogeneous Systems**  
*P. Bastian, O. Ippisch, F. Rezanezhad, H. J. Vogel, K. Roth* ..... 579

**Lake Dynamics: Observation and High-Resolution Numerical Simulation**  
*C. von Rohden, A. Hauser, K. Wunderle, J. Ilmberger, G. Wittum, K. Roth* ..... 599

**Part VIII Computer Visualization**

**Preamble** ..... 623

<b>Advanced Flow Visualization with HiVision</b> <i>S. Bönnisch, V. Heuveline</i> .....	625
<b>VisuSimple: An Interactive Visualization Utility for Scientific Computing</b> <i>Th. Dunne, R. Becker</i> .....	635
<b>Volume Rendering in Scientific Applications</b> <i>S. Krömker, J. Rings</i> .....	653
<b>List of Contributors</b> .....	667

**Mathematical Analysis  
for Transport-Reaction Systems**

---

## Preamble

This chapter contains two articles which are concerned with the theoretical analysis of nonlinear evolution systems.

The first article *“Fluid flows and free boundaries”* gives an overview of results concerning viscous fluids with a free boundary modeling, for example, the motion of water with a water–air interface. The relevant tools and the major problems in the analysis of the corresponding equations are described. The focus is on results that concern existence, analysis of spectra, bifurcation, contact angles, coupling with elastic materials, and asymptotic behavior.

The second article *“Nonlinear evolution equations and applications”* deals with special kinds of evolution processes such as occurring in modeling the interaction of biological species in so-called “gradostats”. The main issues of this study are persistence results for species competition, bifurcations, and coexistence equilibria. Another central aspect is the evolution of shapes if geometry plays a role. Set-valued maps are considered for describing evolution in metric spaces and Aubin’s concept of mutational equations is extended.

---

# Fluid Flows and Free Boundaries\*

B. Schweizer<sup>1</sup>, S. Bodea<sup>2</sup>, C. Surulescu<sup>2</sup>, and I. Surovtsova<sup>2</sup>

<sup>1</sup> Mathematisches Institut, Universität Basel

<sup>2</sup> Institut für Angewandte Mathematik, Universität Heidelberg

**Summary.** We give an overview over results concerning viscous fluids with a free boundary, modelling e.g. the motion of water with a water-air interface. We describe the relevant tools and the major problems in the analysis of the corresponding equations. Our focus are results that concern existence, analysis of spectra, bifurcation, contact angles, coupling with elastic materials, and asymptotic behavior.

## 1 Introduction

Due to their frequent appearance in physical or biological applications, systems involving phase boundaries or multiple-fluid flow are a fastly developing field in mathematical analysis. In this contribution we are concerned with a fluid that is described by the incompressible time-dependent Navier–Stokes equations and which exhibits a free boundary. The difficulty in these problems is that the domain which is occupied by fluid is not given in advance. Instead, the domain in which the equations are satisfied must be determined as a part of the problem.

We start this contribution by sketching the fundamental techniques for existence results in section 2. We will see why spaces of regular function are used and why the results are necessarily local in nature. All this is done for fluid flow in a domain with a free surface and with surface tension included. We will then go beyond the standard setting and describe some of the further results that were achieved within this project. In section 3 we sketch results on the spectrum of the linearized operator and on bifurcations. In section 4 we indicate how the coupling with a second material can be analyzed. We see this contribution also as an opportunity to describe some older results from todays perspective.

---

\*This work has been supported by the German Research Foundation (DFG) through SFB 359 (Project A1) at the University of Heidelberg.

## 2 Existence Theories

In this contribution we will always assume that the domain in which the fluid equations are posed is of a simple form. We denote the unknown domain by  $\Omega = \Omega_t$  and assume that the free boundary can be written as a graph with a height function  $h$ , that is, we consider  $\Omega_t = \{(\tilde{x}, x_3) | H < x_3 < h(\tilde{x}, t)\}$ . We will describe three- as well as two-dimensional results. In order to do so, we let  $x$  denote either a real variable,  $\tilde{x} = x_1 \in \mathbb{R}$ , or a point in the plane,  $\tilde{x} = (x_1, x_2) \in \mathbb{R}^2$ . We will indicate the range of applicability in the results.

The range for  $x$  will be most of the time a bounded domain, that is  $\tilde{x} \in (0, 1)$  or  $\tilde{x} \in (0, 1)^2$ , depending on the dimension. In the case of a bounded domain we assume periodicity conditions on the lateral boundaries, that is, the height extends to a periodic function on  $\mathbb{R}$  (or  $\mathbb{R}^2$ ), and bulk quantities like velocity and pressure also extend to periodic functions in  $x$ . The depth is assumed to be constant, either with a finite value,  $H < 0$ , or set to be  $H = -\infty$ . The Navier–Stokes equations with viscosity  $\nu > 0$  are posed on  $\Omega = \Omega_t$ , in three dimensions

$$\partial_t v - \nu \Delta v + (v \cdot \nabla)v + \nabla p = 0, \quad (1)$$

$$\nabla \cdot v = 0, \quad (2)$$

and the boundary conditions on  $\Gamma = \Gamma_t = \text{graph}(h(\cdot, t))$  are

$$\partial_t h - v_3 + \partial_1 h v_1 + \partial_2 h v_2 = 0, \quad (3)$$

$$\partial_n v_\tau + \partial_\tau v_n = 0, \quad (4)$$

$$p - 2\nu \partial_n v_n + \beta \mathcal{H}(h) = g. \quad (5)$$

Equation (4) must hold for all tangential vectors  $\tau$ , here and below  $n$  is the exterior normal to the domain. In addition, we are given initial values for  $v$  and  $h$ ,

$$v(\cdot, 0) = v_0, \quad h(\cdot, 0) = h_0. \quad (6)$$

In the boundary conditions, equation (3) is the kinematic condition. It expresses that the boundary moves with the fluid and is always parametrized by  $h$ . The equation can be derived by differentiating the relation  $Y(t) = h(X(t), t)$  for Lagrangian coordinates  $(X, Y)$  with respect to time, and using  $\partial_t(X, Y) = (v_1, v_2, v_3)$ . Equations (4) and (5) are the balance of forces on the free boundary for the tangential and the normal components, respectively. The expression  $\mathcal{H}(h)$  stands for the mean curvature of the curve or surface given by  $h$ ,

$$\mathcal{H}(h)(x, t) = \nabla_x \cdot \left( \frac{\nabla_x h(x, t)}{\sqrt{1 + |\nabla_x h(x, t)|^2}} \right).$$

Note that, if applied to  $h$ , the gradient is understood as a gradient in the horizontal ( $\tilde{x}$ -) directions, only. The number  $\beta > 0$  is the physical parameter

for the surface tension. In the case of a finite depth, we impose a no-slip boundary condition on the bottom,  $v = 0$  on the line  $\{x_3 = H\}$ .

Existence theories for the above equations are restricted to local results. They are either local in time or they are results for small initial values (initial domains close to a reference domain and small initial velocity). Judging from current methods, a non-local existence result seems to be out of sight. We will come back to this point in subsection 2.4. But first, we have to sketch the standard approach to existence theories, which is via linearized equations.

## 2.1 Linearizing the Equations

The above system is nonlinear: it contains the convective term, the mean curvature  $\mathcal{H}$  is nonlinear, and the domain depends on the solution. The last point implies that we can not even define a sum of two solutions, since, in general, they live on different domains. The nonlinearity created by the changes in the domain turns out to be of higher order than the other two nonlinearities and poses the main difficulty in existence results. Typically, it is treated as follows. Given an initial domain  $\Omega_0$  which is close to a reference domain  $R$  (we assume in the following that  $R$  is a rectangle), we prescribe how to construct from the height function  $h(\cdot, t)$  a parametrization of the domain  $\Omega_t$  by  $X(\cdot, t) : R \rightarrow \Omega_t$ . Then, in the easiest case, we set

$$\hat{v} : R \times (0, T) \rightarrow \mathbb{R}^3, \quad \hat{v}(x, t) := v(X(t), t), \quad (7)$$

and similar for the pressure  $p$  to find  $\hat{p} : R \rightarrow \mathbb{R}$ . Transforming the differential operators into the  $X$ -coordinates, we find equations for  $\hat{v}$  and  $\hat{p}$  on the rectangle  $R$ , the boundary values are coupled to the unknown  $h$ . The system is now posed on the reference domain  $R$ . We can linearize all terms in the trivial solution and separate linear terms from the higher order terms, collecting the linear terms on the left hand side. Omitting the hat, the equations now read

$$\partial_t v - \nu \Delta v + \nabla p = f, \quad (8)$$

$$\nabla \cdot v = d, \quad (9)$$

with boundary condition on  $\Sigma := \{(x, y) \in \partial R | y = 0\}$ ,

$$\partial_t h - v_3 = g_0, \quad (10)$$

$$\partial_3 v_i + \partial_i v_3 = g_i, \quad i = 1, 2, \quad (11)$$

$$p - 2\nu \partial_3 v_3 + \beta \Delta_x h = g_3. \quad (12)$$

Additionally we have an initial condition for  $v$  and  $h$ . The right hand side has to be understood as nonlinear terms,  $f = f(v, p, h)$ ,  $d = d(v, p, h)$  etc.

## 2.2 Treatment of the Nonlinear Equations

Once we have the nonlinear system in the form (8)–(12), there is a natural choice of an iteration scheme to treat the nonlinearity. One tries to find an existence result and regularity estimates for the linear system (8)–(12) where  $f, \dots, g_3$  are assumed to be given, time-dependent quantities. This defines a solution map  $S : (f, \dots, g_3) \mapsto (v, p, h)$ . An iteration is then constructed by composing the evaluation of the nonlinear terms with the solution operator,

$$(v^k, p^k, h^k) \mapsto (f(v^k, p^k, h^k), \dots, g_3(v^k, p^k, h^k)) \xrightarrow{S} (v^{k+1}, p^{k+1}, h^{k+1}). \quad (13)$$

It is shown for many situations that this iteration is contractive for small  $T > 0$ , i.e. a small time interval.

### *A transformation preserving the solinoidal structure*

The transformation chosen in (7) introduces nonlinear terms in all the equations (8)–(12). We will see that it is desirable in the iteration to have vanishing right hand sides  $d$  and  $g_0$ . One can actually chose a transformation replacing (7) such that  $d = 0$  and  $g_0 = 0$ . This transformation was exploited e.g. in [1], [5], [7], [8], [10]. One sets  $J := \det DX$  and

$$\hat{v}(x) := J(x)(DX(x))^{-1} \cdot v(X(x)). \quad (14)$$

One may show with a direct calculation that  $\hat{v}$  is again divergence-free. A calculation which provides more insight and which is much shorter exploits that  $\hat{v}$  can be interpreted as the pull-back of a differential form. In three dimensions one identifies  $v$  with the closed 2-form  $V = v_1(dy_2 \wedge dy_3) + v_2(dy_3 \wedge dy_1) + v_3(dy_1 \wedge dy_2) =: v \cdot dS_y$ . We can then define  $\hat{v}$  as the coefficients of the form  $\hat{V} := X^*V = \hat{v} \cdot dS_x$ . As a pull-back,  $\hat{V}$  is again a closed form and thus  $\hat{v}$  is divergence-free. In order to calculate the coefficients, we use an arbitrary 1-form  $\lambda = \lambda_1 dy_1 + \lambda_2 dy_2 + \lambda_3 dy_3$  to calculate two pull-backs under  $X$ ,

$$\begin{aligned} V \wedge \lambda &= \sum_i v_i \lambda_i dy_1 \wedge dy_2 \wedge dy_3, \\ X^*(V \wedge \lambda) &= \sum_j v_j \lambda_j J dx_1 \wedge dx_2 \wedge dx_3, \\ X^*(V \wedge \lambda) &= X^*V \wedge X^*\lambda = (\hat{v} dS_x) \wedge \sum_{j,k} \lambda_j \partial_k X_j dx_k = \sum_{j,k} \hat{v}_k \lambda_j \partial_k X_j. \end{aligned}$$

Comparing the last two expressions we find (14) for  $\hat{v}$ .

As indicated, this transformation has actually a second advantage. If the parametrization  $X$  is chosen with  $X_1(x_1, x_2, x_3) = x_1$  and  $X_2(x_1, x_2, x_3) = x_2$ , then, at the upper boundary of the rectangle, where  $X_3(x_1, x_2, 0) = h(x_1, x_2)$ ,

$$DX = \begin{pmatrix} 1 & 0 & 0 \\ 0 & 1 & 0 \\ \partial_1 h & \partial_2 h & \partial_3 X_3 \end{pmatrix}, \quad DX^{-1} = \frac{1}{\partial_3 X_3} \begin{pmatrix} \partial_3 X_3 & 0 & 0 \\ 0 & \partial_3 X_3 & 0 \\ -\partial_1 h & -\partial_2 h & 1 \end{pmatrix}.$$

Hence the vertical component of  $\hat{v}$  is

$$\hat{v}_3 = (-\partial_1 h, -\partial_2 h, 1) \cdot v,$$

which transforms (3) into  $\partial_t h = \hat{v}_3$ , and thus we have  $g_0 = 0$  in (10). We will see in the next subsection that vanishing nonlinearities  $d$  and  $g_0$  mean a great simplification if we want to make the iteration (13) well-defined and contractive.

### 2.3 Estimates for the Linearized System

The method described above restricts us in the choice of function spaces. In order to have well defined evaluations such as  $(v, p, h) \mapsto f$  in (13), we must seek solutions in spaces of regular functions. In order to have energy estimates (or Fourier methods) available, we chose the scale of Sobolev spaces  $H^k = W^{k,2}$  based on the Hilbert spaces  $L^2$ .

A typical choice of function spaces is the following. With  $r \in \mathbb{N}$  we seek for  $v(t) \in H^r(R)$ ,  $p(t) \in H^{r-1}(R)$ , and  $h(t) \in H^{r+1/2}(\Sigma)$  for almost every  $t \in (0, T)$ . With this choice, we can associate to each small height function  $h(\cdot, t)$  a parametrization  $X(\cdot, t) \in H^{r+1}(R)$ . By choosing the natural number  $r$  large enough, we achieve that the evaluation of all nonlinear terms is well defined. For large  $r$  ( $r > 3$  in three space dimensions) we additionally achieve that the order of the nonlinearity coincides with the maximal number of derivatives. For example, if the nonlinearity contains second derivatives of  $v$  and only first derivatives of  $X$ , then the nonlinearity defines a map  $H^r \times H^{r+1/2} \rightarrow H^{r-2}$ .

#### *Energy estimates*

The estimates for the linear system are always based on the following observation which exploits the energy estimates for the linearized system. Let us assume that  $(v, p, h)$  solves the linear system on the bounded rectangle  $R$ . We assume that we have performed a Fourier-Transform in time such that the differential operator  $\partial_t$  is replaced by the multiplication with  $\lambda \in \mathbb{R}$ , which is the dual variable to time. To have transparent calculations, we assume to have a general  $f$ , but vanishing right hand sides in the other equations and  $\nu = 1$ .

Since the boundary conditions in (11) and (12) contain entries of the symmetrized gradient  $Dv := [\nabla v + (\nabla v)^T]/2$ , we use  $Dv$  also in integrations by parts. Multiplication of (11), that is, of  $\lambda v - \Delta v + \nabla p = f$  with  $v$  and integrating over  $R$  yields

$$\lambda \int_R |v|^2 + 2 \int_R |Dv|^2 + \int_\Sigma n \cdot (p - 2Dv) \cdot v = \int_R f v. \quad (15)$$

Inserting the boundary conditions (11) and (12), which take the form  $e_3 \cdot (p - 2Dv) = -\beta \Delta_x h e_3$ , we find

$$\lambda \int_R |v|^2 + 2 \int_R |Dv|^2 - \int_\Sigma \beta \Delta_x h v_3 = \int_R f v. \quad (16)$$

Using now (10) in the form  $v_3 = \lambda h$  and with a multiplication by  $\lambda$  we have

$$\lambda^2 \|v\|_{L^2(R)}^2 + 2\lambda \int_R |Dv|^2 + \lambda^2 \beta \int_\Sigma |\nabla_x h|^2 \leq \|\lambda v\|_{L^2(R)} \|f\|_{L^2(R)}. \quad (17)$$

This provides the resolvent estimate

$$\|v\|_{L^2(R)} + \|h\|_{H^1(\Sigma)} \leq \frac{1}{\lambda} \|f\|_{L^2(R)}. \quad (18)$$

In order to have additionally regularity estimates, one first differentiates equation (11) in a horizontal ( $\tilde{x}$ -) direction, and then multiplies with  $v$ . Korn's inequality yields  $L^2(R)$ -estimates for all second derivatives of  $v$  if at least one derivative is in tangential direction. This provides the desired regularity of boundary values of  $v$ . We can therefore exploit the regularity results for the stationary Stokes system  $-\Delta v + \nabla p = f - \lambda v$  which imply  $\|v\|_{H^2} + \|p\|_{H^1} \leq C\|f - \lambda v\|_{L^2}$ . At this stage one finally determines the regularity of the height function  $h$ . Since  $\Delta_x h$  coincides with (a sum of) traces of  $p$  and first derivatives of  $v$ , we have  $\Delta_x h \in H^{1/2}(\Sigma)$  and hence

$$\|v\|_{H^2} + \|p\|_{H^1} + \|h\|_{H^{2+1/2}(\Sigma)} \leq C\|f\|_{L^2}. \quad (19)$$

By differentiating with respect to horizontal directions more than once, one can raise the power of the Sobolev space by any natural number.

### *Interpretations of the Energy Estimates*

Based on inequalities (18) and (19) there are different ways to construct solutions to the linear equations with maximal regularity. Beale carries out in [1] the concept of a Fourier-transform in time. In this setting, regularity estimates and resolvent estimates for the Fourier-transform  $\tilde{v} : \mathbb{R} \rightarrow L^2(R, \mathbb{R}^n)$  yield corresponding estimates for the solution,

$$\begin{aligned} (\lambda \mapsto \tilde{v}(\lambda)) \in L^2(\mathbb{R}, H^2(R, \mathbb{R}^n)) &\Rightarrow v \in L^2(\mathbb{R}, H^2(R, \mathbb{R}^n)), \\ (\lambda \mapsto \lambda \tilde{v}(\lambda)) \in L^2(\mathbb{R}, L^2(R, \mathbb{R}^n)) &\Rightarrow \partial_t v \in L^2(\mathbb{R}, L^2(R, \mathbb{R}^n)). \end{aligned}$$

As such, these implications hold for smooth maps that vanish on the negative time-axis. In order to deal with general initial values, extensions of the initial values with maximal regularity must exist.

Another approach is to phrase the problem in the language of semigroup theory. There are two difficulties to be circumvented. One problem is that no time derivative of the pressure appears in the equations. To deal with this problem one can use the operator of harmonic extensions. Let us denote by

$$\mathcal{P} : H^{r+1/2}(\Sigma) \rightarrow H^{r+1}(R), \quad \varphi \mapsto u, \quad \text{where } \Delta u = 0, \quad u|_\Sigma = \varphi,$$

such that  $u$  vanishes on the bottom and has a periodic extension. In the linear equations (we assume  $\nabla \cdot f = 0$  for simplicity), we find that the pressure  $p$  is harmonic. Equation (12) with  $g_3 = 0$  then allows to replace everywhere  $p$  by  $\mathcal{P}(2\nu\partial_3 v_3 - \beta\Delta_x h)$ . We set

$$\mathcal{L} \begin{pmatrix} v \\ h \end{pmatrix} := \begin{pmatrix} -\Delta v + \nabla \mathcal{P}(2\nu\partial_3 v_3 - \beta\Delta_x h) \\ -v_3|_{\Sigma} \end{pmatrix}.$$

By choosing a space of divergence-free functions (here we exploit  $d = 0$ ) and incorporating (11) through the choice of the domain of  $\mathcal{L}$ , the problem takes the form

$$\frac{d}{dt} \begin{pmatrix} v \\ h \end{pmatrix} + \mathcal{L} \begin{pmatrix} v \\ h \end{pmatrix} = \begin{pmatrix} f \\ g_0 \end{pmatrix}. \quad (20)$$

After these formal manipulations there appears a problem concerning the orders of differentiability. If we demand the base-space to be of the form  $H^r(R) \times H^{r+1/2}(\Sigma)$ , then we can invert  $\mathcal{L}$  only on subspaces of the form  $H^{r-2}(R) \times H^{r-1/2}(\Sigma)$ . A way to deal with this problem is to exploit that also the right hand side in the second row,  $g_0$ , vanishes. With semigroup methods one can show

**Theorem 1.** *The operator  $\mathcal{L}$  generates an analytic semigroup on a subspace of  $X^r := H^r(R) \times H^{r+1/2}(\Sigma)$ . Solutions of (20) with  $g_0 = 0$  and compatible initial values satisfy for  $f \in C^\alpha([0, T], X^r)$  maximal regularity estimates,*

$$(v, h) \in C^\alpha([0, T], X^{r+2}) \cap C^{1+\alpha}([0, T], X^r).$$

*For  $r \geq 2$  there exists a solution to the nonlinear equations in the same function spaces.*

We refer to [8] for a proof.

It may be of advantage to keep all proofs as elementary as possible. In fact, Renardy avoids in [7] both the Fourier-transform and the semigroup theory. He finds energy estimates in the primary variables without using a variable  $\lambda$ . Instead, estimates for  $\lambda v$  are expressed as estimates for  $\partial_t v$ , and the multiplication of the equation with  $\lambda$  is replaced by a differentiation of the equation with respect to time. The existence of solutions is then shown with a time-discretized approximation.

## 2.4 Obstacles to Existence Theories

So far, we have outlined the *standard approach* to existence results for free boundary problems in fluid equations. We would like to emphasize that the quoted articles deal with additional topics and have goals beyond the sketched existence proof. In [1] an unbounded domain is treated. This introduces additional difficulties, e.g. Korn's inequality fails in this case. In [7] an inflow condition is considered. This reduces the maximal regularity and we can not, as assumed above, increase the order of differentiability to arbitrary order by differentiating in a tangential direction. We come back to this point below. In [8], the semigroup methods are a tool to prove a Hopf-bifurcation theorem.

*On the existence of solutions far from equilibrium*

We have claimed before that an existence result 'in the large' seems to be out of reach. We can now explain this statement concerning the standard approach sketched above. The standard approach needs function spaces of high regularity in order to have the nonlinearities well-defined as maps between the related function spaces. In [7] it was desirable to decrease the regularity as much as possible. Renardy achieved a result in which  $h(t) \in H^{3/2}(\Sigma)$  is bounded for all  $t$  in the two-dimensional case (compare Theorem 9 of [7]). But this means, that  $h(t)$  must still be Hölder continuous at all times.

Without smallness assumption on the initial data one can perform the following thought-experiment. Starting from a dumbbell shaped drop with a very thin neck, surface tension will create a high pressure within the neck. The fluid is pushed out and a pinch-off is expected. Indeed, calculations in [4] confirm this believe by providing a self-similar solution with pinch-off in finite time. In the moment of the topology change, the surface loses its regularity and the standard method fails. We can not even solve the problem by performing surgery: The geometry at the moment of the pinch-off, re-parametrized over two topological balls and interpreted as new initial values, does not provide the regularity that is needed for initial values in the standard approach. In particular, we can not expect regular a priori estimates beyond pinch-off.

*Regularity questions in the contact angle problem*

Less severe are the regularity problems in the contact angle problem. Still, the standard approach does not work in this case. Let us first describe the questions concerning the dynamic contact angle. In the easiest setting we study a two-dimensional domain with independent spatial variables  $(x, y) \in \mathbb{R}^2$ . If the fluid is in contact with a solid material, say, at  $x = 0$  and at  $x = 1$ , we have to pose conditions other than periodicity on the lateral walls  $\Sigma_1 = \{(x, y) \in \bar{\Omega} | x = 0\}$  and  $\Sigma_2 = \{(x, y) \in \bar{\Omega} | x = 1\}$ . A good choice turns out to be (for some  $\gamma_1 = -\gamma_2 \in \mathbb{R}$ )

$$v_1 = 0 \quad \text{on } \Sigma_i, \quad i = 1, 2, \quad (21)$$

$$\partial_x v_2 - \gamma_i v_2 = 0 \quad \text{on } \Sigma_i, \quad i = 1, 2. \quad (22)$$

The first condition asserts that the fluid can not penetrate the wall, the second condition is the general Navier-slip condition in which the tangential velocity is proportional to the tangential stress across the wall. In order to complete the system it remains to pose boundary conditions for  $h$ , one choice is to consider a fixed angles

$$\partial_x h(0) = -\partial_x h(1) = \alpha, \quad (23)$$

where  $\alpha = \tan(90^\circ - \Theta_0)$  and  $\Theta_0$  is the constant contact angle. Equation (1)–(5) together with (21)–(23) are a complete set of equations for the dynamic contact point problem.

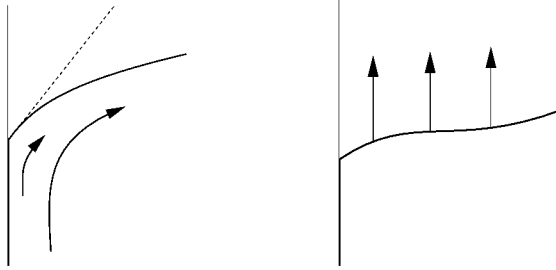


**Fig. 1.** Flow field near the contact point, stationary and instationary case

The reason to use (22) instead of the no-slip condition  $v_2 = 0$  (formally,  $\gamma_i = \infty$ ) is that there are no solutions of finite energy (finite  $H^1$ -norm) if we seek for  $v_2 \neq 0$  on the upper surface and  $v_2 = 0$  on  $\Sigma_i$ . The regularization with the Navier-slip condition is standard in the context of coating problems.

After the regularization we can expect a better regularity of the solutions. But let us perform a formal calculation that indicates that one must be careful in expecting too much. Let us assume that we can evaluate all functions below in the point of contact  $(x, y) = (0, h(0, t))$ , and that derivatives commute. We then find

$$\begin{aligned} 0 &= \partial_t \alpha = \partial_t \partial_x h(0, h(0)) = \partial_x \partial_t h(0, h(0)) \\ &= \partial_x v_2(0, h(0)) = \gamma_1 v_2(0, h(0)). \end{aligned}$$

This means that the point of contact can not move, which is in contrast to physical experience (compare Figure 1; note that there is no problem in the stationary flow problem). On a mathematical level we find that we can not expect any estimates for  $v(t) \in H^2(R)$ .

In particular we find: even with the regularization of the Navier-slip condition, the standard approach to an existence result will fail. The regularity properties of solutions can not be increased by differentiating with respect to  $x$ , since then the boundary condition on  $\Sigma_i$  are lost. We can not hope for regularity estimates for  $v(t)$  in  $H^r(R)$  for  $r \geq 2$ .

Nevertheless, there is a positive statement for the dynamic contact angle problem, at least for a special choice of  $\Theta_0$ .

**Theorem 2.** *For  $\Theta_0 = 90^\circ$ ,  $\gamma_1 = -\gamma_2 > 0$ , and compatible small initial values  $(v_0, h_0)$ , there is a short time interval  $(0, T)$  and a solution to the contact angle problem on  $(0, T)$ .*

For the precise statement and the choice of function spaces we refer to [10]. To our knowledge, until today, this is the only well-posedness result for the dynamic contact angle problem.

The proof of Theorem 2 consists in bringing together two facts.

1.) Renardy developed in [7] a method that allows to show existence results

for free boundary fluid problems exploiting only the regularity  $v(t) \in H^s$ ,  $s \in (1, 2)$ .

2.) In the case  $\Theta_0 = 90^\circ$  a reflection principle can be used to find resolvent estimates for the linear equations. To be more precise, one decomposes solutions of the linearized equation into a solution of a free boundary problem with  $\partial_x v_2|_{\Sigma_i} = 0$ , and a solution of a Stokes problem for given  $\partial_x v_2|_{\Sigma_i}$ . The first contribution can be reflected across  $\Sigma_i$  to give a periodic solution, and the standard technique can be employed. An interpolation yields optimal estimates for the solution in  $H^s$  for  $s \in (1, 2)$ . Together with maximal regularity results for the second contribution, one finds the resolvent estimates for the linear equations. The technique of Renardy allows to treat the nonlinear problem.

### 3 Eigenvalues and Bifurcations

#### 3.1 Eigenvalues of the Linearized Free Boundary System

With  $\mathcal{L}$  being the generator of the linearized free boundary Stokes system, we now ask:

Can we characterize the spectrum of the operator  $\mathcal{L}$ ?

In this context it is helpful to use the language of semigroup theory and to write the linearized system in the form (20). But we want to emphasize that this is only a convenient way to state results. One can as well use the original (homogeneous) linearized system (8)–(12) and investigate the following question:

Can we characterize all values of  $\lambda \in \mathbb{C}$  such that a solution of the form

$$(v(x, y, t), p(x, y, t), h(x, y, t)) = (v_0(x, y), p_0(x, y), h_0(x, y)) e^{\lambda t}.$$

exists for the linearized time-dependent problem?

An investigation of the operator  $\mathcal{L}$  shows that, on a bounded spatial domain  $R$ , the operator  $\mathcal{L}^{-1}$  is compact, hence the spectrum of  $\mathcal{L}$  consists of eigenvalues. In particular, the two questions above are indeed equivalent. Furthermore, the operator  $\mathcal{L}$  is a positive operator and every eigenvalue has a positive real part.

Let us first interpret the physical meaning of eigenvalues. A real eigenvalue  $\lambda \in \mathbb{R}$  is necessarily positive and corresponds to an overdamped motion, i.e. to a solution that decays exponentially in a self-similar way without changing the sign of the similarity factor. Instead, a non-real eigenvalue corresponds to an oscillatory behavior. From physical reasoning we in fact expect such a behavior. Let us assume that we start with a sinusoidal height function  $h$ . The surface tension leads to a high pressure in the crest and a low pressure in the

trough. The fluid is accelerated and develops a flow-profile which corresponds to a transport of mass from the crest to the trough. The height-profile now flattens. If the process is fast enough, then the wave reaches in finite time a state with flat height-profile and with a nontrivial flow profile. In this case, the sinusoidal shape of the height-function reappears with inverted sign, i.e. with the positions of crest and trough exchanged. The process repeats and leads to oscillations. We expect such oscillations if the surface tension is large enough in order to flatten out the wave in finite time.

The physical intuition is correct as can be shown with mathematical analysis. The following result was shown in two space dimensions in [8] and in three space dimensions in [2]. In both cases, periodicity conditions are used in one horizontal direction. In [2], on the lateral walls a slip condition was used and a vanishing normal derivative of the height function, i.e. equations (21)–(22) with  $\gamma_1 = \gamma_2 = 0$  and (23) with  $\Theta_0 = 0$ .

**Theorem 3.** *For each wave number  $k \in \mathbb{Z}$  (or  $k \in \mathbb{Z}^2$  in three dimensions) there exists a critical value for the surface tension  $\beta_0(k)$  such that the following is true: For  $0 < \beta \leq \beta_0(k)$  all eigenvalues with wave number  $k$  (the  $x$ -dependence is  $e^{ikx}$ ) are real and positive. For  $\beta > \beta_0(k)$  there is a pair of conjugate complex nonreal eigenvalues with wave number  $k$ .*

We next indicate the main ideas in the proof which relies on a comparison of the free-boundary system with two auxiliary Stokes systems. For notational convenience we give formulas for the two-dimensional case.

1.) *Decomposition into invariant subspaces.* All eigenfunctions can be written in the form

$$v(x, y) = V(y)e^{ikx}, \quad p(x, y) = P(y)e^{ikx}, \quad h(x) = e^{ikx}, \quad \text{with } k \in \mathbb{Z}.$$

This can be shown as follows: For fixed  $k$ , functions of the above form constitute a subspace  $X_k$  of the chosen function space  $X$ , and the operator  $\mathcal{L}$  maps the subspace  $X_k$  into itself. We have thus found a decomposition of the base-space into a family of closed invariant subspaces. Since the span of the  $(X_k)_{k \in \mathbb{Z}}$  is all of  $X$ , the spectrum of  $\mathcal{L}$  is the union of the eigenvalues of the operators  $\mathcal{L}_k := \mathcal{L}|_{X_k} : X_k \rightarrow X_k$ .

2.) *Characterization of eigenvalues.* We next characterize eigenvalues  $\lambda \in \mathbb{C}$  of the operator  $\mathcal{L}_k$  with the help of the Stokes system. We write down the eigenvalue problem for  $\mathcal{L}$  by looking at equations (8)–(12) in two dimensions, leaving out equation (12) at this point. We thus consider

$$-\lambda v - \nu \Delta v + \nabla p = 0, \tag{24}$$

$$\nabla \cdot v = 0, \tag{25}$$

$$v_2|_{\Sigma} = -\lambda h, \tag{26}$$

$$\partial_2 v_1 + \partial_1 v_2 = 0. \tag{27}$$

This is a Stokes system and we assume periodicity conditions on the lateral walls and a no-slip condition on the bottom. The system is solvable for given

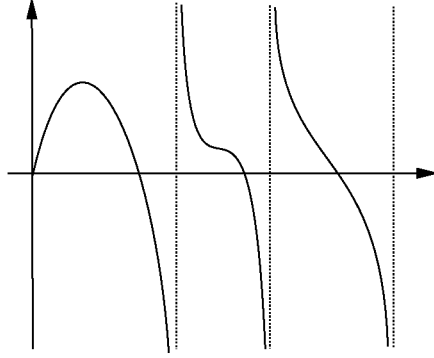


Fig. 2. The function  $g_k$  on the real axis

$h$  except if  $\lambda$  is one of the positive real eigenvalues of the Stokes operator with Dirichlet boundary conditions on  $\Sigma$ . We denote the solution  $(v, p)$  of the system (24)–(27) with  $h(x) = \Phi_0(x) := e^{ikx}$  by  $(v, p) = S_k(\lambda)$ . We can now give a characterization of eigenvalues of  $\mathcal{L}$ . A number  $\lambda \in \mathbb{C}$  is an eigenvalue of  $\mathcal{L}_k$ , if the remaining equation (12) is satisfied, that is, if

$$(p - 2\nu\partial_2 v_2)|_{\Sigma} = g_k(\lambda) \Phi_0 = \beta k^2 \Phi_0 \quad \text{holds for } (v, p) = S_k(\lambda). \quad (28)$$

It is therefore enough to study the relation  $g_k(\lambda) = \beta k^2$ .

3.) *Properties of the function  $g_k$ .* It remains to observe that the function  $g_k$  can be described well, at least on the real axis. One can read off easily from equation (26), which contains the only right hand side in the Stokes system, that for  $\mathbb{R}_+ \ni \lambda \rightarrow 0$  we find  $g_k(\lambda) \rightarrow 0$ . Furthermore, for each eigenvalue  $\lambda_N$  with wave number  $k$  of the (Neumann-) Stokes operator, we find  $g_k(\lambda_N) = 0$ , since there is a nontrivial solution with vanishing normal force in (28). One can furthermore calculate that for eigenvalues  $\lambda_D$  of the (Dirichlet-) Stokes operator, we find  $|g_k(\lambda)| \rightarrow \infty$  for  $\lambda \rightarrow \lambda_D$ . More detailed investigations reveal the signs of  $g_k$  in the various limits and that  $g_k$  can have at most one turning point in each interval between two neighboring (Dirichlet-) Stokes eigenvalues. This provides a complete understanding of the function  $g_k$  on the real axis; it is illustrated in Figure 2.

We can now read off for which real values of  $\lambda$  we have an eigenvalue of  $\mathcal{L}_k$ . For vanishing surface tension, equation (28) is satisfied in the zeros of  $g_k$ , that is, in 0 and in the (Neumann-) Stokes eigenvalues. If  $\beta \geq 0$  is increased, the first two eigenvalues move towards another, all the other eigenvalues move to the left. At a critical point of the surface tension, the first two eigenvalues meet and necessarily leave the real axis.

The analysis can actually be extended to a system with a forcing term. A model for the effect of wind on the free surface of water is obtained by introducing in (5) the right hand side  $g = \gamma \partial_x h$ . In this model, the effect of

the wind is an additional normal force on the wind-facing sides of the wave. For every value of  $\gamma \in \mathbb{R}$ , this forced system is again tractable with the above method. The following result is shown in [8] and [2] for two and three space dimensions, respectively.

**Theorem 4.** *For every value of surface tension  $\beta > 0$  and every wave number  $k \in \mathbb{Z}$  (or  $k \in \mathbb{Z}^2$  in three dimensions), there exists a critical value for the wind-force  $\gamma_0(k)$  such that for  $\gamma > \gamma_0$  there is a pair of conjugate complex purely imaginary eigenvalues. In dependence of  $\gamma$ , they cross the imaginary axis transversally.*

The essential part of the proof was done for Theorem 3. Let us assume that for the given  $k \in \mathbb{Z}$  the surface tension  $\beta$  is above the critical values, that is, we have exactly two non-real eigenvalues. A continuation of the function  $g_k$  into the complex plane reveals that for  $\gamma > 0$  the real eigenvalues (corresponding to  $h(x) = e^{ikx}$ ) all move to the lower half of the complex plane (the conjugate complex eigenvalues correspond to the function  $h(x) = e^{-ikx}$ ). For small  $\gamma > 0$  we therefore have one complex eigenvalue in the upper half-plane, all other eigenvalues in the lower half-plane. The same situation appears if we start with a surface tension  $\beta$  below the critical value, since the derivative of  $g_k$  has the negative sign in the first eigenvalue and the positive sign in the other eigenvalues.

It now suffices to show that eigenvalues can not be real for  $\gamma > 0$ , which follows again by a study of the function  $g_k$ . For the isolated eigenvalue in the upper half plane one shows that it can not escape to infinity with non-negative real part. Since it can neither merge with other eigenvalues nor return to the real axis, this eigenvalue must cross the imaginary axis. We refer again to [8] and [2] for details and for the transversality result.

### 3.2 Bifurcation Analysis and Travelling Waves

We have already mentioned after Theorem 1 that a Hopf-bifurcation theorem can be shown with the help of semigroup theory. Theorem 4 provides the existence of imaginary eigenvalues for a critical wind-speed  $\gamma_0$ . The two results together allow to conclude the existence of a branch of non-trivial solutions to equations (1)–(5) for each  $\beta > 0$ . Parametrizing over a signed wave height  $\varepsilon \in \mathbb{R}$ , we find a branch of parameters  $\gamma_\varepsilon$  extending the critical wind-force  $\gamma_0$  and non-trivial time-periodic solutions  $u_\varepsilon = (v_\varepsilon, p_\varepsilon, h_\varepsilon)$  of the nonlinear system (1)–(5) with  $g = \gamma_\varepsilon \partial_x h_\varepsilon$ .

The invariance of the nonlinear equations imply that these solutions are in fact translations, i.e. we have found travelling wave solutions of the nonlinear equations. Therefore, there exists a wave-speed  $c_\varepsilon \in \mathbb{R}$  such that  $\partial_t u_\varepsilon = c_\varepsilon \partial_x u_\varepsilon$ . A numerical analysis allows to determine the bifurcation diagram ( $\varepsilon$  versus  $\gamma_\varepsilon$ ) and the diagram for wave-speeds ( $\varepsilon$  versus  $c_\varepsilon$ ), see Figure 3. We refer to [11] for details and for an analysis of quantitative properties of the nonlinear solutions.

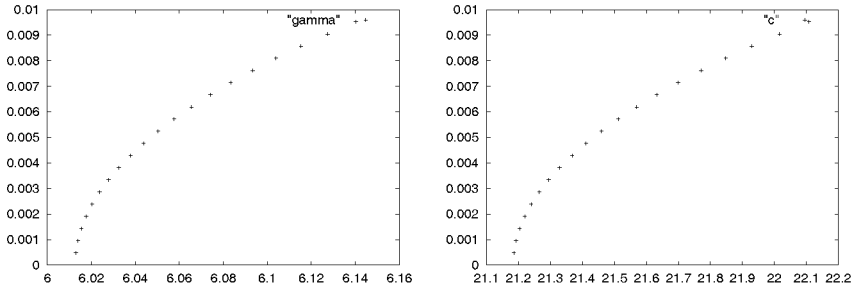


**Fig. 3.** The bifurcation diagram and values for the wave-speed

## 4 Coupling with Other Materials

So far, we studied the flow of a viscous fluid in a time-dependent domain. Deformations of the domain gave a feed-back to the fluid in two ways: Firstly, a change of the domain changes the flow geometry. Secondly, surface tension creates a normal force on the boundary which has the effect that curved boundaries try to straighten out. This is a model for the following physical situation: water is in contact with air, and, due to its low density, we can neglect the effect of the air.

In this section we describe some results that deal with the opposite case that we can not neglect the effect of the second material. This is the case for a water-air system in the case of high velocities (subsection 4.1), and for fluid flow coupled to an elastic material (subsections 4.2 – 4.4).

### 4.1 Coupling with an Inviscid Fluid

There are many contributions regarding the coupling with a second viscous fluid, and we do not intend to describe these results here. Instead, we wish to describe the situation where the second fluid (e.g. air) is a much less viscous fluid, such that the description with inviscid equations is desirable. In this case, the Navier–Stokes equations for the water as in (1)–(5) are coupled with the incompressible Euler equations in the domain  $\tilde{\Omega}_t$  above the free surface. We consider the two-dimensional case, write  $(x, y)$  for the spatial co-ordinates and  $\tilde{\Omega}_t = \{(x, y) | y > h(x, t)\}$ . The equations in  $\tilde{\Omega}_t$  are

$$\begin{aligned} \partial_t v + (v \cdot \nabla)v + \frac{1}{\rho} \nabla q &= 0, \\ \nabla \cdot v &= 0, \end{aligned}$$

where  $\rho > 0$  is the density of the inviscid fluid. In the boundary condition (5) one must set  $g = q$ , that is, the force felt by the water equals the pressure of the air near the free boundary. Additionally, initial conditions for  $v$  and  $h$ , and boundary conditions must be posed.

In [22] a local existence result for this system (with  $\beta = 0$ ) is derived under the assumption that the density  $\rho$  is small. The result of [9] is a local existence result without the smallness assumption on  $\rho$ . In the case of a small density, one can utilize an iteration scheme of the following form:

1. For a given force  $g$  acting on the free boundary, solve the free boundary problem for the viscous fluid with force  $g$ .
2. The solution yields a time-evolution of the domain. Solve the Euler equations in this time-dependent domain to find anew force-field  $g$ .

An iteration of these steps yields the desired solution. The iteration is contractive if the density  $\rho$  is small.

For general  $\rho$ , we can not expect the above iteration to converge. The physical argument is that we assumed that the effect of the inviscid fluid is small and that it can be treated as a small perturbation of the system without air. The method works for small densities or small velocities. A generalization of the existence result must employ a new iteration scheme. We emphasize that this also gives a hint on how to construct a numerical method.

Every acceleration of the free boundary necessarily induces an acceleration of the inviscid fluid, and inertia leads to a pressure distribution on the free boundary that hinders the acceleration. If the velocities (or the density) are small, this is a small effect. Else, we have to incorporate this effect in the treatment of the single-fluid problem. The idea is to anticipate a simplified version of the inertia term in the iteration scheme. For a given boundary evolution  $h(t)$  and a velocity field  $v(t) : \Gamma(t) \rightarrow \mathbb{R}^2$  we define  $\Phi : \tilde{\Omega}_t \rightarrow \mathbb{R}$  and  $\tilde{v}$ ,

$$\tilde{v} := \nabla \Phi \quad \text{with} \quad \Delta \Phi(t) = 0,$$

with the boundary condition

$$\partial_n \Phi = v \cdot n \quad \text{on} \quad \Gamma(t).$$

For a detailed description of other boundary conditions and the normalization of  $\Phi$  we refer to [9]. We can now define a pressure field  $\tilde{q}(t) := -\rho \partial_t \Phi$ . With these definitions we find

$$\partial_t \tilde{v} + \frac{1}{\rho} \nabla \tilde{q} = 0,$$

in  $\tilde{\Omega}_t$  and  $\tilde{v} \cdot n = v \cdot n$  on  $\Gamma(t)$ . Hence  $\tilde{v}$  and  $\tilde{q}$  satisfy the Euler equations except for the convective term.

The iteration scheme to solve the nonlinear problem is the following.

1. Solve the single-fluid free boundary problem with the functional relation  $g = \tilde{q}(h, v)$ , with  $\tilde{q}$  as defined above. Exploit in the resolvent estimates that  $\tilde{q}$  is a positive term.
2. Solve the Euler equations in the given geometry to find the pressure  $q$ . Exploit that the correction  $q - \tilde{q}$  is a compact perturbation compensating the lower order term of the convective derivative.

This scheme provides a fixed-point iteration with a compact iteration map. The Schauder fixed-point theorem yields the existence of a solution to the nonlinear problem.

### 4.2 Stationary Flow Coupled with an Elastic Material

We are interested in the flow of a viscous fluid in a domain with elastic walls. This physical problem appears for instance in the modeling of blood-flow, where the blood fills the arteries that are described as elastic tubes (see e.g. [6] for related model equations). In [19] such a three-dimensional fluid-elastic structure interaction problem is studied. The fluid is described by the incompressible Navier-Stokes equations and flows inside a smooth elastic cylinder with thickness.

As in the free boundary systems above, the fluid domain is unknown and the flow deforms the boundary. This deformation gives a two-fold feed-back to the fluid, the change of domain and via forces. In the case of the interaction with an elastic material, the exerted forces are of a complex nature. The changes of the fluid domain must be interpreted as deformation (Dirichlet-) conditions for the elastic material. The bulk equations for the material (modeled as a three-dimensional structure) determine the normal and tangential forces on the boundary which are the second feed-back to the fluid. The fluid equations (1)–(2) are coupled with the bulk equation for the deformation  $u$  of the elastic material,

$$-\nabla \cdot T_P(u) = g, \tag{29}$$

which holds in the domain occupied by the elastic material,  $T_P$  is the first Piola-Kirchhoff stress tensor and  $g$  the exterior bulk forces. The coupling to the fluid is via the following replacement of conditions (3)–(5) on  $\Gamma(t)$ ,

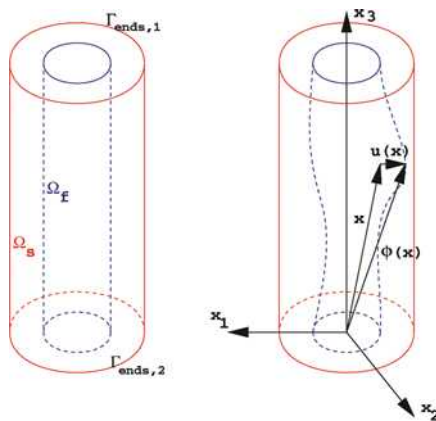


Fig. 4. Description of the flow-domain

$$v = 0 \tag{30}$$

$$T_P(u) \cdot n = pn - \nu(\nabla v + (\nabla v)^T) \cdot n. \tag{31}$$

Note that now both equations are vector valued, since the elastic material requires also tangential boundary conditions. For precise conditions at the other boundaries we refer to [21].

The problem in the description of this coupled system concerns coordinates. While for the elastic problem Lagrange coordinates are appropriate, velocity and stress of the fluid are described in Eulerian coordinates. In the balance of forces in equation (31) this means that the derivative on the right hand side is understood in Eulerian coordinates and must be converted into Lagrange coordinates with the cofactor matrix of the gradient of the transformation  $\text{Id} + u$  of the elastic material.

The results of [19]–[21] are existence results for the coupled system. As explained in section 2, these are necessarily results for small deformations and for smooth applied force-fields. The elastic structure is modeled as a St.Venant-Kirchhoff material and the geometry is as indicated in Figure 4. Different boundary conditions at the inflow and outflow sides were considered. In [20] a periodicity condition is assumed for the fluid and the elastic material. In [19] clamped elastic walls are considered and the proof exploits a reflection principle. The generality of the boundary conditions is improved in [21].

### 4.3 Instationary Flow Coupled with an Elastic Material

The next step was to study the time-dependent case. It turned out that in the instationary case the coupling of two three-dimensional media is not accessible with the above methods. Therefore, the elastic wall was described by a lower dimensional set of equations – in the case of elastic materials this means to describe the wall with plate equations.

In [18] a time-dependent 3D-2D fluid-elastic structure interaction problem was studied. It can be formulated in the following way: a viscous, incompressible fluid flows through a box having an elastic plate as cover, the bottom and two opposite lateral walls are rigid, the other two opposite lateral walls are the inflow and the outflow boundary, respectively. The fluid domain changes with time and must be determined as part of the problem. The fluid is now described by the time-dependent Navier-Stokes equations with prescribed pressures on the inflow and outflow parts of the boundary. These are nonstandard boundary conditions for a fluid flow, which constitutes the main difference with [3], where a similar problem has been considered, but where all lateral boundaries of the fluid domain were rigid. The elastic structure is viewed as a thin plate which is clamped at its boundary.

One of the results in [18] is a local existence theorem for the coupled system. The proof utilizes an auxiliary problem in which the convective term is regularized. This problem is linearized and the linearized equations are solved with Galerkin’s method. A generalized Schauder fixed point theorem

due to Zeidler yields the existence of a solution to the nonlinear auxiliary problem. The passage to the limit in the regularization parameter eventually yields a solution to the full coupled system.

#### 4.4 A One-Dimensional Model for Fluid-Structure Interaction

In this section we sketch an alternative approach to describe the flow in a compliant vessel. This is the one-dimensional model which reduces the problem of the fluid-structure interaction to the equations similar to the Euler equations of gas dynamics ([14]–[17]).

The velocity profile of the fluid in an compliant vessel depends on the Womersley number  $\alpha^2 = a^2 \frac{\omega}{\nu}$ , where  $a$  is the tube radius and  $\omega$  the circular frequency (see [6], for instance). At high Womersley numbers, the velocity profile is flat over most of the vessel and has a thin boundary layer at the wall. At very low  $\alpha$ , the flow is essentially quasi static Poiseuille flow at each instant.

A one-dimensional model was derived in [14] by averaging the Navier–Stokes equations (1)–(2) for axialsymmetrical flow on the assumptions

$$\frac{a}{L} \ll 1, \quad \frac{1}{\alpha^2} \ll 1,$$

so that the influence of the viscous boundary layer on the mean flow can be neglected (here  $L$  is the characteristic length of a tube). The conservation of mass and momentum requires:

$$\frac{\partial S}{\partial t} + \frac{\partial (S u)}{\partial x} = 0, \quad \frac{\partial u}{\partial t} + u \frac{\partial u}{\partial x} + \frac{1}{\rho} \frac{\partial p}{\partial x} = 0,$$

where  $x$  is now a one-dimensional variable and denotes the longitudinal position within the tube,  $u(t, x)$  and  $p(t, x)$  denote the average axial velocity and average pressure over the cross-section, and  $S(t, x)$  is the two-dimensional volume of the cross-section. The compliance of the wall has an effect corresponding to the compressibility in gas dynamics. For the details of model justification, we refer to [14],[15].

This model was applied to the blood flow in large arteries and studied both analytically (by the method of characteristics) and numerically. Surovtsova examined some features of solutions connected with the steeping of compression waves, leading to the possible formation of shock waves. They can occur in the human aorta, for instance, because of some cardiovascular illnesses (e.g. increase of vessel wall distensibility and some ventricles abnormalities). It was shown that the viscoelasticity of the vessel wall has a much larger influence on the damping of shock waves than the blood viscosity.

For studying the mechanical effects caused by the local stiffening of an artery (due to the vascular prosthesis or stent, for example), a modified one-dimensional model was derived in [16], [17]. The artery was supposed to be an orthotropical thin elastic shell composed of different homogeneous materials.

The solution was obtained by matched asymptotic expansions. The results proved the high flexure concentration close to the compliance jump. It can initiate an adaptive response in the vascular tissue (e.g. the restenosis). The use of orthotropical graft may reduce the peak value of these shear forces to a remarkable extent. Other features of the solution are the reflection of blood from the suture, as well as the pressure increase in the more rigid prosthesis (see [16], [17] for details).

## References

1. J.T. Beale. Large time regularity of viscous surface waves. *Arch. Rat. Mech. Anal.*, 84:307–352, 1984.
2. S. Bodea. *Oscillations of a Fluid in a Channel*. Dissertationsschrift an der Universität Heidelberg, 2004.
3. A. Chambolle, B. Desjardins, M.J. Esteban, C. Grandmont, *Existence of Weak Solutions for an Unsteady Fluid-Plate Interaction Problem*, Cahier du CEREMADE 0245 (2002).
4. J. Eggers. Theory of drop formation. *Phys. Fluids* 7, 5:941–953, 1995.
5. J.G. Heywood. On uniqueness questions in the theory of viscous flow. *Acta Math.*, 136:237–246, 1976.
6. A. Quarteroni, M. Tuveri, A. Veneziani, *Computational vascular fluid dynamics: Problems, models and methods*, Comput. Vis. Sci. 2, No.4 (2000), 163-197.
7. M. Renardy. An existence theorem for a free surface flow problem with open boundaries. *Comm. Part. Diff. Eq.*, 17:1387–1405, 1992.
8. B. Schweizer. Free boundary fluid systems in a semigroup approach and oscillatory behavior. *SIAM J. Math. Anal.*, 28:1135–1157, 1997.
9. B. Schweizer. A two-component flow with a viscous and an inviscid fluid. *Comm. PDE*, 25:887–901, 2000.
10. B. Schweizer. A well-posed model for dynamic contact angles. *Nonlinear Analysis TMA*, 43:109–125, 2001.
11. B. Schweizer. Bifurcation analysis for surface waves generated by wind. *SIAM J. Appl. Math.*, 62:407–423, 2001.
12. B. Schweizer. A stable time discretization of the Stefan problem with surface tension. *SIAM J. Numer. Anal.*, 40:1184–1205, 2002.
13. B. Schweizer. On the three-dimensional Euler equations with a free boundary driven by surface tension. *Annales de l'Institut Henri Poincaré (C) Analyse Non Linéaire*, 22(6):753–781, 2005.
14. I. Surovtsova. Blood flow in large vessels: A one-dimensional model. University Heidelberg, Preprint 2002-08 (SFB 359) (2002)
15. I. Surovtsova. Application of the one-dimensional model for blood flow to the vascular prosthesis. In: Capasso, V. (ed.) *Mathematical Modelling & Computing in Biology and Medicine*. The MIRIAM Project Series, Progetto Leonardo, ESCULAPIO Pub. Co., Bologna, Italy, pp: 242-248 (2003)
16. I. Surovtsova. Application of the one-dimensional model for blood flow through vascular prosthesis. University Heidelberg, Preprint 2003-04 (SFB 359) (2003)
17. I. Surovtsova. Effects of compliance mismatch on blood flow in an artery with endovascular prosthesis. *Journal of Biomechanics* (accepted).